

## Supporting Information

### [Ln<sub>16</sub>] Complexes (Ln = Gd<sup>III</sup>, Dy<sup>III</sup>): Molecular Analogues of Natural Minerals such as Hydrotalcite

Paul Richardson,<sup>a</sup> Ting-Jung Hsu,<sup>b</sup> Che-Jung Kuo,<sup>b</sup> Rebecca J. Holmberg,<sup>a</sup> Bulat Gabidullin,<sup>a</sup> Mathieu Rouzières,<sup>c,d</sup> Rodolphe Clérac,<sup>c,d\*</sup> Muralee Murugesu<sup>a\*</sup> and Po-Heng Lin<sup>b\*</sup>

<sup>a</sup>Department of Chemistry and Biomolecular Sciences, University of Ottawa, ON, Canada, K1N 6N5. Email: m.murugesu@uottawa.ca; Fax: +1 (613) 562 5170; Tel: +1 (613) 562 5800 ext. 2733

<sup>b</sup>Department of Chemistry, National Chung Hsing University, 250 Kuo Kang Rd., Taichung 402, Taiwan R.O.C.

<sup>c</sup>CNRS, CRPP, UMR 5031, Pessac 33600, France.

<sup>d</sup>Univ. Bordeaux, CRPP, UMR 5031, Pessac 33600, France

## Table of Contents

	<b>Experimental Section</b>	<b>S3</b>
<b>Table S1.</b>	Crystallographic data for compounds <b>1</b> and <b>2</b> .	<b>S4</b>
<b>Table S2.</b>	Selected bond distances for <b>1</b> .	<b>S5</b>
<b>Table S3.</b>	Selected bond angles for <b>1</b> .	<b>S6</b>
<b>Table S4.</b>	Selected bond distances for <b>2</b> .	<b>S9</b>
<b>Table S5.</b>	Selected bond angles for <b>2</b> .	<b>S10</b>
<b>Figure S1.</b>	Coordination mode of $\text{bsc}^{2-}$ ligands in <b>1</b> and <b>2</b> ( $\text{Ln} = \text{Gd}^{\text{III}}$ , <b>1</b> ; $\text{Dy}^{\text{III}}$ , <b>2</b> ).	<b>S12</b>
<b>Table S6.</b>	SHAPE analysis for all nine-coordinate metals in <b>1</b> and <b>2</b> .	<b>S13</b>
<b>Table S7.</b>	SHAPE analysis for all eight-coordinate metals in <b>1</b> and <b>2</b> .	<b>S13</b>
<b>Table S8.</b>	SHAPE analysis for all seven-coordinate metals in <b>1</b> and <b>2</b> .	<b>S14</b>
<b>Figure S2.</b>	Field dependence of the magnetization as $M$ vs $H$ (left) and $M$ vs $H/T$ (right) plots for <b>1</b> between 1.8 and 8 K with sweep-rates of 100 – 600 Oe/min. The solid lines are guides for the eyes.	<b>S14</b>
<b>Figure S3.</b>	Field dependence of the magnetization as $M$ vs $H$ (left) and $M$ vs $H/T$ (right) plots for <b>2</b> between 1.8 and 8 K with sweep-rates of 100 – 600 Oe/min. The solid lines are guides for the eyes.	<b>S15</b>
<b>Figure S4.</b>	Frequency dependence of the real ( $\chi'$ , top) and imaginary ( $\chi''$ , bottom) components of the ac susceptibility in zero-dc field at different temperatures between 1.8 and 2.7 K for a polycrystalline sample of <b>2</b> .	<b>S15</b>
<b>Figure S5.</b>	Frequency dependence of the real ( $\chi'$ , top) and imaginary ( $\chi''$ , bottom) components of the ac susceptibility at 1.9 K at different dc fields between 0 and 1 T for a polycrystalline sample of <b>2</b> .	<b>S16</b>

## Experimental Details

### Materials

Chemicals were purchased from Alfa Aesar and Strem and were used without further purification. H<sub>2</sub>bsc was synthesized according to a previously reported procedure.<sup>1</sup> Reactions for the synthesis of **1** and **2** were performed under aerobic/ambient conditions.

### Synthesis

[Et<sub>4</sub>N]<sub>3</sub>[Gd<sub>16</sub>(μ<sub>3</sub>-OH)<sub>24</sub>(bsc)<sub>6</sub>(H<sub>2</sub>O)<sub>18</sub>]Cl<sub>15</sub>·2H<sub>2</sub>O·EtOH (**1**): Compound **1** was synthesized in an analogous manner to **2**, yielding the hexadecanuclear complex [Et<sub>4</sub>N]<sub>3</sub>[Gd<sub>16</sub>(μ<sub>3</sub>-OH)<sub>24</sub>(bsc)<sub>6</sub>(H<sub>2</sub>O)<sub>18</sub>]Cl<sub>15</sub>·xH<sub>2</sub>O in 21% yield after one week. IR (KBr plates, cm<sup>-1</sup>): 3381 (s), 1620 (s), 1548 (m), 1475 (m), 1438 (m), 1396 (m), 1293 (m), 1205 (m), 1154 (w), 1063 (w), 1036 (w), 1001 (w), 964 (w), 921 (w), 904 (w), 841 (w), 764 (w), 643 (w), 595 (w). Elemental analysis (%). Calcd: C, 22.87; H, 3.28; N, 6.21. Found: C, 23.11; H, 3.63; N, 6.34.

[Et<sub>4</sub>N]<sub>3</sub>[Dy<sub>16</sub>(μ<sub>3</sub>-OH)<sub>24</sub>(bsc)<sub>6</sub>(H<sub>2</sub>O)<sub>18</sub>]Cl<sub>15</sub>·2H<sub>2</sub>O·EtOH (**2**): To a suspension of DyCl<sub>3</sub>·6H<sub>2</sub>O (0.189 g, 0.5 mmol) and H<sub>2</sub>bsc (0.075 g, 0.25 mmol) in EtOH/THF (2:1 ratio) was added 0.5 mmol of [Et<sub>4</sub>NH][OH] (35 wt. % in H<sub>2</sub>O). The resulting yellow solution was stirred, filtered, and left to slowly evaporate, which lead to the isolation of light yellow crystals of [Et<sub>4</sub>N]<sub>3</sub>[Dy<sub>16</sub>(μ<sub>3</sub>-OH)<sub>24</sub>(bsc)<sub>6</sub>(H<sub>2</sub>O)<sub>18</sub>]Cl<sub>15</sub>·xH<sub>2</sub>O in 23.6% yield after one week. IR (KBr plates, cm<sup>-1</sup>): 3481 (br), 1627 (br), 1550 (s), 1477 (s), 1438 (s), 1394(br), 1328 (s), 1299 (s), 1209 (m), 1155 (m), 1126 (w), 1066 (m), 1037 (m), 1002 (w), 966 (w), 923 (w), 904 (w), 842 (w), 815 (m), 804 (m), 771 (s), 644 (m), 617 (m), 595 (m), 580 (m), 567 (m), 549 (m), 528 (m), 518 (m), 486 (w), 472 (m), 459 (m), 443 (m), 420 (m), 397 (m), 385 (w). Elemental analysis (%). Calcd: C, 22.40; H, 3.14; N, 6.08. Found: C, 22.11; H, 3.59; N, 5.99.

CCDC 1849319 - 1849320 contain the supplementary crystallographic data for this paper. These data can be obtained free of charge from The Cambridge Crystallographic Data Centre via [www.ccdc.cam.ac.uk/data\\_request/cif](http://www.ccdc.cam.ac.uk/data_request/cif)

### Physical Measurements

**X-ray crystallography.** Single-crystal X-ray diffraction (SCXRD) data collection results for compound **1** and **2** were collected on a Bruker AXS SMART single crystal diffractometer with a sealed Mo tube APEX II CCD detector, which was used to collect the unit cell and intensity data using graphite Mo-Kα radiation (λ = 0.71073 Å).<sup>2</sup> Data reduction included correction for Lorentz and polarisation effects, with an applied multi-scan absorption correction (SADABS).<sup>3</sup> Crystal structures were solved and refined using SHELXTL.<sup>4</sup> All non-hydrogen atoms were refined with anisotropic thermal parameters. Hydrogen atom positions were calculated geometrically and were riding on their respective atoms. When viewing the crystal structure, Cl73, Cl74, and Cl77 are all fully occupied, while Cl72, Cl75 and Cl76 are partially occupied. The occupancy of these specific Cl<sup>-</sup> anions is refined using the SUMP<sup>5</sup> command and is constrained to six per complex. The crystal lattice of **2** contains large solvent accessible voids, which are filled with highly disordered solvent molecules. The electron density of these molecules was accounted for using the SQUEEZE routine from the PLATON<sup>6</sup> software package.

**FT-IR spectroscopy.** Infrared spectra were recorded on all samples in the solid state under ambient conditions on a Nicolet iS5 FT-IR spectrometer in the 4000-400  $\text{cm}^{-1}$  region. The background of the environment was eliminated by OMNIC software.

**Magnetic measurements.** Magnetic measurements were performed using a Quantum Design SQUID magnetometer MPMS-XL7, operating between 1.8 and 300 K for dc-applied fields ranging from -7 to 7 T. Susceptibility measurements were performed on a freshly filtered polycrystalline sample of **1** and **2** (10.34 and 11.90 mg, respectively), covered with mineral oil for **2** (15.82 mg) and sealed in polypropylene bag (size and mass:  $3 \times 0.5 \times 0.02$  cm; 19.95 and 23.90 mg, respectively). Direct current (dc) susceptibility measurements were performed at 0.1 and 1 T. Alternating current (ac) susceptibility measurements were performed under an oscillating ac field between and 1 and 10 Oe, with ac frequencies ranging from 10-10000 Hz. An  $M$  vs  $H$  measurement was carried out at 100 K to confirm the absence of ferromagnetic impurities. The magnetic data were corrected for the sample holder, mineral oil and intrinsic diamagnetic contributions.

**Table S1** Crystallographic data for compounds **1** and **2**.

Compound	<b>1</b>	<b>2</b>
Empirical formula	$\text{C}_{114}\text{H}_{200}\text{Cl}_{15}\text{Gd}_{16}\text{N}_{27}\text{O}_{64}$	$\text{C}_{114}\text{H}_{188}\text{Cl}_{15}\text{Dy}_{16}\text{N}_{27}\text{O}_{67}$
Crystal system	Trigonal	Trigonal
Space group	$R\bar{3}$	$R\bar{3}$
$a$ (Å)	36.144(4)	35.8327(7)
$b$ (Å)	36.144(4)	35.8327(7)
$c$ (Å)	28.831(3)	28.8733(7)
$\alpha$ (°)	90	90
$\beta$ (°)	90	90
$\gamma$ (°)	120	120
$V$ (Å <sup>3</sup> )	32619(8)	32106.0(15)
$Z$	6	6
$\rho_{\text{calc}}$ (g $\text{cm}^{-3}$ )	1.837	1.904
$\lambda$ (Å)	0.71073	0.71073
$T$ (K)	200(2)	200(2)
$\mu$ ( $\text{mm}^{-1}$ )	5.059	5.769
$F(000)$	17148	17412
Reflections collected	131710	83286
Independent reflections	17336	24776
Reflections with $I > 2\sigma(I)$	12288	15341
Goodness of fit on $F^2$	1.086	1.039
$R_1, wR_2$ ( $I > 2\sigma(I)$ ) <sup>a</sup>	0.0578, 0.1397	0.0608, 0.1432
$R_1, wR_2$ (all data)	0.0900, 0.1758	0.1112, 0.1862

<sup>a</sup> $R = R_1 = \sum ||F_o| - |F_c|| / \sum |F_o|$ ;  $wR_2 = \{ \sum [w(F_o^2 - F_c^2)^2] / \sum [w(F_o^2)^2] \}^{1/2}$ ;  $w = 1 / [\sigma^2(F_o^2) + (ap)^2 + bp]$ , where  $p = [\max(F_o^2, 0) + 2F_c^2] / 3$ .

**Table S2** Selected bond distances for **1**.

Bond	Distance (Å)	Bond	Distance (Å)
Gd(1)-O(1)	2.372(7)	Gd(3)-N(35)	2.561(8)
Gd(1)-O(58)	2.386(7)	Gd(4)-O(56)	2.368(6)
Gd(1)-O(47)	2.391(6)	Gd(4)-O(43) <sup>b</sup>	2.369(7)
Gd(1)-O(44)	2.410(9)	Gd(4)-O(57)	2.390(6)
Gd(1)-O(46)	2.427(8)	Gd(4)-O(1)	2.403(7)
Gd(1)-O(48)	2.454(6)	Gd(4)-O(54) <sup>b</sup>	2.410(6)
Gd(1)-O(45)	2.504(9)	Gd(4)-O(47)	2.439(7)
Gd(1)-O(11)	2.544(7)	Gd(4)-O(58)	2.445(6)
Gd(1)-N(8)	2.566(8)	Gd(4)-O(53) <sup>b</sup>	2.506(7)
Gd(2)-O(22)	2.247(7)	Gd(5)-O(57) <sup>a</sup>	2.308(6)
Gd(2)-O(21)	2.271(8)	Gd(5)-O(57) <sup>b</sup>	2.308(6)
Gd(2)-O(48)	2.402(7)	Gd(5)-O(57)	2.308(6)
Gd(2)-O(49)	2.427(6)	Gd(5)-O(55)	2.361(17)
Gd(2)-O(33)	2.464(6)	Gd(5)-O(56)	2.384(7)
Gd(2)-O(11)	2.465(7)	Gd(5)-O(56) <sup>b</sup>	2.384(7)
Gd(2)-N(13)	2.623(8)	Gd(5)-O(56) <sup>a</sup>	2.384(7)
Gd(2)-N(30)	2.648(9)	Gd(6)-O(56) <sup>a</sup>	2.366(6)
Gd(3)-O(53)	2.374(6)	Gd(6)-O(47)	2.398(7)
Gd(3)-O(43)	2.399(7)	Gd(6)-O(49)	2.409(6)
Gd(3)-O(51)	2.401(8)	Gd(6)-O(48)	2.409(7)
Gd(3)-O(54)	2.430(7)	Gd(6)-O(54)	2.410(6)
Gd(3)-O(49)	2.454(6)	Gd(6)-O(58)	2.410(6)
Gd(3)-O(52)	2.465(8)	Gd(6)-O(57)	2.417(7)
Gd(3)-O(50)	2.477(9)	Gd(6)-O(53)	2.422(7)
Gd(3)-O(33)	2.531(7)		

Symmetry transformations used to generate equivalent atoms: <sup>a</sup> -y+1, x-y+1, z; <sup>b</sup> -x+y, -x+1, z

**Table S3** Selected bond angles for **1**.

Bond	Angle (°)	Bond	Angle (°)
O(1)-Gd(1)-O(58)	72.8(2)	O(54)-Gd(3)-O(33)	67.0(2)
O(1)-Gd(1)-O(47)	70.9(2)	O(49)-Gd(3)-O(33)	64.9(2)
O(58)-Gd(1)-O(47)	61.3(2)	O(52)-Gd(3)-O(33)	126.3(3)
O(1)-Gd(1)-O(44)	106.0(3)	O(50)-Gd(3)-O(33)	130.1(3)
O(58)-Gd(1)-O(44)	131.4(3)	O(53)-Gd(3)-N(35)	133.3(3)
O(47)-Gd(1)-O(44)	72.3(3)	O(43)-Gd(3)-N(35)	69.5(3)
O(1)-Gd(1)-O(46)	136.7(3)	O(51)-Gd(3)-N(35)	79.1(3)
O(58)-Gd(1)-O(46)	135.5(3)	O(54)-Gd(3)-N(35)	84.2(3)
O(47)-Gd(1)-O(46)	145.9(3)	O(49)-Gd(3)-N(35)	127.1(2)
O(44)-Gd(1)-O(46)	79.3(3)	O(52)-Gd(3)-N(35)	77.5(3)
O(1)-Gd(1)-O(48)	142.4(2)	O(50)-Gd(3)-N(35)	144.4(3)
O(58)-Gd(1)-O(48)	76.5(2)	O(33)-Gd(3)-N(35)	62.2(2)
O(47)-Gd(1)-O(48)	75.5(2)	O(56)-Gd(4)-O(43)#2	135.8(2)
O(44)-Gd(1)-O(48)	78.7(3)	O(56)-Gd(4)-O(57)	72.2(2)
O(46)-Gd(1)-O(48)	80.9(3)	O(43)#2-Gd(4)-O(57)	108.5(2)
O(1)-Gd(1)-O(45)	74.1(3)	O(56)-Gd(4)-O(1)	122.8(2)
O(58)-Gd(1)-O(45)	144.6(3)	O(43)#2-Gd(4)-O(1)	87.3(2)
O(47)-Gd(1)-O(45)	118.0(3)	O(57)-Gd(4)-O(1)	137.9(2)
O(44)-Gd(1)-O(45)	70.4(3)	O(56)-Gd(4)-O(54)#2	73.7(2)
O(46)-Gd(1)-O(45)	67.4(3)	O(43)#2-Gd(4)-O(54)#2	74.1(2)
O(48)-Gd(1)-O(45)	138.8(3)	O(57)-Gd(4)-O(54)#2	130.4(2)
O(1)-Gd(1)-O(11)	120.7(2)	O(1)-Gd(4)-O(54)#2	91.2(2)
O(58)-Gd(1)-O(11)	67.1(2)	O(56)-Gd(4)-O(47)	74.4(2)
O(47)-Gd(1)-O(11)	119.7(2)	O(43)#2-Gd(4)-O(47)	149.7(2)
O(44)-Gd(1)-O(11)	133.2(3)	O(57)-Gd(4)-O(47)	79.4(2)
O(46)-Gd(1)-O(11)	68.6(3)	O(1)-Gd(4)-O(47)	69.6(2)
O(48)-Gd(1)-O(11)	63.8(2)	O(54)#2-Gd(4)-O(47)	123.8(2)
O(45)-Gd(1)-O(11)	122.1(3)	O(56)-Gd(4)-O(58)	123.6(2)
O(1)-Gd(1)-N(8)	70.4(3)	O(43)#2-Gd(4)-O(58)	95.0(2)
O(58)-Gd(1)-N(8)	81.7(3)	O(57)-Gd(4)-O(58)	68.7(2)
O(47)-Gd(1)-N(8)	132.6(3)	O(1)-Gd(4)-O(58)	71.3(2)
O(44)-Gd(1)-N(8)	145.3(3)	O(54)#2-Gd(4)-O(58)	160.0(2)
O(46)-Gd(1)-N(8)	81.4(3)	O(47)-Gd(4)-O(58)	59.9(2)

O(48)-Gd(1)-N(8)	126.0(3)	O(56)-Gd(4)-O(53)#2	69.0(2)
O(45)-Gd(1)-N(8)	75.7(3)	O(43)#2-Gd(4)-O(53)#2	68.8(2)
O(11)-Gd(1)-N(8)	62.2(3)	O(57)-Gd(4)-O(53)#2	74.6(2)
O(1)-Gd(1)-Gd(6)	99.73(16)	O(1)-Gd(4)-O(53)#2	146.1(2)
O(22)-Gd(2)-O(21)	113.2(3)	O(54)#2-Gd(4)-O(53)#2	60.0(2)
O(22)-Gd(2)-O(48)	88.6(3)	O(47)-Gd(4)-O(53)#2	140.0(2)
O(21)-Gd(2)-O(48)	156.9(2)	O(58)-Gd(4)-O(53)#2	132.3(2)
O(22)-Gd(2)-O(49)	157.6(3)	O(57)#1-Gd(5)-O(57)#2	117.71(9)
O(21)-Gd(2)-O(49)	87.7(3)	O(57)#1-Gd(5)-O(57)	117.71(9)
O(48)-Gd(2)-O(49)	72.1(2)	O(57)#2-Gd(5)-O(57)	117.71(9)
O(22)-Gd(2)-O(33)	124.8(3)	O(57)#1-Gd(5)-O(55)	81.21(17)
O(21)-Gd(2)-O(33)	75.6(2)	O(57)#2-Gd(5)-O(55)	81.21(17)
O(48)-Gd(2)-O(33)	85.9(2)	O(57)-Gd(5)-O(55)	81.21(17)
O(49)-Gd(2)-O(33)	66.3(2)	O(57)#1-Gd(5)-O(56)	146.4(2)
O(22)-Gd(2)-O(11)	75.0(3)	O(57)#2-Gd(5)-O(56)	76.2(2)
O(21)-Gd(2)-O(11)	125.5(3)	O(57)-Gd(5)-O(56)	73.4(2)
O(48)-Gd(2)-O(11)	65.7(2)	O(55)-Gd(5)-O(56)	132.31(16)
O(49)-Gd(2)-O(11)	86.6(2)	O(57)#1-Gd(5)-O(56)#2	76.2(2)
O(33)-Gd(2)-O(11)	146.0(2)	O(57)#2-Gd(5)-O(56)#2	73.4(2)
O(22)-Gd(2)-N(13)	75.1(3)	O(57)-Gd(5)-O(56)#2	146.4(2)
O(21)-Gd(2)-N(13)	68.7(3)	O(55)-Gd(5)-O(56)#2	132.31(16)
O(48)-Gd(2)-N(13)	127.4(3)	O(56)-Gd(5)-O(56)#2	79.6(2)
O(49)-Gd(2)-N(13)	107.4(3)	O(57)#1-Gd(5)-O(56)#1	73.4(2)
O(33)-Gd(2)-N(13)	144.0(3)	O(57)#2-Gd(5)-O(56)#1	146.4(2)
O(11)-Gd(2)-N(13)	61.8(3)	O(57)-Gd(5)-O(56)#1	76.2(2)
O(22)-Gd(2)-N(30)	67.7(3)	O(55)-Gd(5)-O(56)#1	132.31(16)
O(21)-Gd(2)-N(30)	76.6(3)	O(56)-Gd(5)-O(56)#1	79.6(2)
O(48)-Gd(2)-N(30)	106.8(3)	O(56)#2-Gd(5)-O(56)#1	79.6(2)
O(49)-Gd(2)-N(30)	127.9(2)	O(56)#1-Gd(6)-O(47)	76.1(2)
O(33)-Gd(2)-N(30)	61.7(2)	O(56)#1-Gd(6)-O(49)	144.0(2)
O(11)-Gd(2)-N(30)	142.3(3)	O(47)-Gd(6)-O(49)	138.9(2)
N(13)-Gd(2)-N(30)	112.0(3)	O(56)#1-Gd(6)-O(48)	123.0(2)
O(53)-Gd(3)-O(43)	70.6(2)	O(47)-Gd(6)-O(48)	76.2(2)
O(53)-Gd(3)-O(51)	147.6(3)	O(49)-Gd(6)-O(48)	72.3(2)
O(43)-Gd(3)-O(51)	136.1(3)	O(56)#1-Gd(6)-O(54)	73.8(2)
O(53)-Gd(3)-O(54)	61.6(2)	O(47)-Gd(6)-O(54)	123.1(2)

O(43)-Gd(3)-O(54)	73.2(2)	O(49)-Gd(6)-O(54)	77.3(2)
O(51)-Gd(3)-O(54)	134.1(3)	O(48)-Gd(6)-O(54)	81.5(2)
O(53)-Gd(3)-O(49)	77.0(2)	O(56)#1-Gd(6)-O(58)	126.9(2)
O(43)-Gd(3)-O(49)	143.1(2)	O(47)-Gd(6)-O(58)	60.9(2)
O(51)-Gd(3)-O(49)	80.6(3)	O(49)-Gd(6)-O(58)	86.6(2)
O(54)-Gd(3)-O(49)	76.1(2)	O(48)-Gd(6)-O(58)	76.9(2)
O(53)-Gd(3)-O(52)	111.9(3)	O(54)-Gd(6)-O(58)	156.2(2)
O(43)-Gd(3)-O(52)	72.2(2)	O(56)#1-Gd(6)-O(57)	74.5(2)
O(51)-Gd(3)-O(52)	71.6(3)	O(47)-Gd(6)-O(57)	79.7(2)
O(54)-Gd(3)-O(52)	144.7(2)	O(49)-Gd(6)-O(57)	113.0(2)
O(49)-Gd(3)-O(52)	138.5(2)	O(48)-Gd(6)-O(57)	144.6(2)
O(53)-Gd(3)-O(50)	73.7(3)	O(54)-Gd(6)-O(57)	133.7(2)
O(43)-Gd(3)-O(50)	111.0(3)	O(58)-Gd(6)-O(57)	68.8(2)
O(51)-Gd(3)-O(50)	78.1(3)	O(56)#1-Gd(6)-O(53)	70.5(2)
O(54)-Gd(3)-O(50)	130.9(3)	O(47)-Gd(6)-O(53)	143.2(2)
O(49)-Gd(3)-O(50)	75.2(3)	O(49)-Gd(6)-O(53)	77.0(2)
O(52)-Gd(3)-O(50)	69.5(3)	O(48)-Gd(6)-O(53)	135.9(2)
O(53)-Gd(3)-O(33)	121.3(2)	O(54)-Gd(6)-O(53)	61.2(2)
O(43)-Gd(3)-O(33)	118.9(2)	O(58)-Gd(6)-O(53)	132.1(2)
O(51)-Gd(3)-O(33)	67.4(3)	O(57)-Gd(6)-O(53)	76.9(2)

Symmetry transformations used to generate equivalent atoms: #1  $-y+1, x-y+1, z$ ; #2  $-x+y, -x+1, z$



**Table S4** Selected bond distances for **2**.

Bond	Distance (Å)	Bond	Distance (Å)
Dy(1)-O(1)	2.346(6)	Dy(3)-N(35)	2.536(8)
Dy(1)-O(59)	2.361(6)	Dy(4)-O(58)	2.343(6)
Dy(1)-O(60)	2.362(6)	Dy(4)-O(59)	2.366(6)
Dy(1)-O(62)	2.383(7)	Dy(4)-O(51)	2.376(6)
Dy(1)-O(63)	2.413(9)	Dy(4)-O(60)	2.378(5)
Dy(1)-O(50)	2.424(6)	Dy(4)-O(55)	2.380(6)
Dy(1)-O(61)	2.485(9)	Dy(4)-O(50)	2.381(6)
Dy(1)-O(22)	2.524(7)	Dy(4)-O(57)	2.387(6)
Dy(1)-N(9)	2.530(8)	Dy(4)-O(56)	2.399(6)
Dy(2)-O(23)	2.229(7)	Dy(5)-O(43)	2.334(6)
Dy(2)-O(21)	2.236(7)	Dy(5)-O(58)#2	2.335(5)
Dy(2)-O(50)	2.373(6)	Dy(5)-O(1)	2.359(6)
Dy(2)-O(51)	2.397(6)	Dy(5)-O(57)	2.371(6)
Dy(2)-O(22)	2.433(6)	Dy(5)-O(55)#2	2.380(6)
Dy(2)-O(44)	2.442(6)	Dy(5)-O(59)	2.409(6)
Dy(2)-N(13)	2.596(8)	Dy(5)-O(60)	2.413(6)
Dy(2)-N(31)	2.614(8)	Dy(5)-O(56)#2	2.487(6)
Dy(3)-O(56)	2.331(6)	Dy(6)-O(57)#2	2.272(5)
Dy(3)-O(52)	2.368(7)	Dy(6)-O(57)	2.272(5)
Dy(3)-O(43)#1	2.381(6)	Dy(6)-O(57)#1	2.272(5)
Dy(3)-O(55)	2.401(6)	Dy(6)-O(58)#2	2.341(6)
Dy(3)-O(53)	2.439(7)	Dy(6)-O(58)#1	2.341(6)
Dy(3)-O(51)	2.445(6)	Dy(6)-O(58)	2.341(6)
Dy(3)-O(54)	2.457(9)	Dy(6)-O(64)	2.357(15)
Dy(3)-O(44)	2.505(6)		

Symmetry transformations used to generate equivalent atoms: #1 -y+1, x-y+1, z; #2 -x+y, -x+1, z

**Table S5** Selected bond angles for **2**.

Bond	Angle (°)	Bond	Angle (°)
O(1)-Dy(1)-O(59)	70.7(2)	O(55)-Dy(3)-O(44)	66.9(2)
O(1)-Dy(1)-O(60)	72.9(2)	O(53)-Dy(3)-O(44)	127.3(2)
O(59)-Dy(1)-O(60)	61.5(2)	O(51)-Dy(3)-O(44)	64.62(19)
O(1)-Dy(1)-O(62)	136.2(2)	O(54)-Dy(3)-O(44)	129.2(3)
O(59)-Dy(1)-O(62)	145.9(2)	O(56)-Dy(3)-N(35)	134.2(2)
O(60)-Dy(1)-O(62)	136.2(2)	O(52)-Dy(3)-N(35)	79.0(3)
O(1)-Dy(1)-O(63)	107.1(3)	O(43)#1-Dy(3)-N(35)	70.3(2)
O(59)-Dy(1)-O(63)	72.4(3)	O(55)-Dy(3)-N(35)	85.0(2)
O(60)-Dy(1)-O(63)	131.3(3)	O(53)-Dy(3)-N(35)	77.5(3)
O(62)-Dy(1)-O(63)	78.3(3)	O(51)-Dy(3)-N(35)	127.3(2)
O(1)-Dy(1)-O(50)	142.2(2)	O(54)-Dy(3)-N(35)	143.7(3)
O(59)-Dy(1)-O(50)	75.41(19)	O(44)-Dy(3)-N(35)	62.7(2)
O(60)-Dy(1)-O(50)	76.6(2)	O(58)-Dy(4)-O(59)	75.56(19)
O(62)-Dy(1)-O(50)	81.6(2)	O(58)-Dy(4)-O(51)	144.40(19)
O(63)-Dy(1)-O(50)	77.4(3)	O(59)-Dy(4)-O(51)	139.0(2)
O(1)-Dy(1)-O(61)	74.1(3)	O(58)-Dy(4)-O(60)	126.59(18)
O(59)-Dy(1)-O(61)	116.3(3)	O(59)-Dy(4)-O(60)	61.2(2)
O(60)-Dy(1)-O(61)	145.2(3)	O(51)-Dy(4)-O(60)	86.6(2)
O(62)-Dy(1)-O(61)	67.3(3)	O(58)-Dy(4)-O(55)	73.55(18)
O(63)-Dy(1)-O(61)	69.7(4)	O(59)-Dy(4)-O(55)	122.3(2)
O(50)-Dy(1)-O(61)	138.1(3)	O(51)-Dy(4)-O(55)	77.9(2)
O(1)-Dy(1)-O(22)	121.0(2)	O(60)-Dy(4)-O(55)	156.53(19)
O(59)-Dy(1)-O(22)	119.8(2)	O(58)-Dy(4)-O(50)	122.7(2)
O(60)-Dy(1)-O(22)	67.2(2)	O(59)-Dy(4)-O(50)	76.1(2)
O(62)-Dy(1)-O(22)	69.1(2)	O(51)-Dy(4)-O(50)	72.2(2)
O(63)-Dy(1)-O(22)	131.8(3)	O(60)-Dy(4)-O(50)	77.1(2)
O(50)-Dy(1)-O(22)	63.8(2)	O(55)-Dy(4)-O(50)	81.4(2)
O(61)-Dy(1)-O(22)	123.7(3)	O(58)-Dy(4)-O(57)	74.04(19)
O(1)-Dy(1)-N(9)	70.9(2)	O(59)-Dy(4)-O(57)	79.9(2)
O(59)-Dy(1)-N(9)	133.1(2)	O(51)-Dy(4)-O(57)	113.4(2)
O(60)-Dy(1)-N(9)	82.1(2)	O(60)-Dy(4)-O(57)	69.13(19)
O(62)-Dy(1)-N(9)	80.9(3)	O(55)-Dy(4)-O(57)	133.33(19)
O(63)-Dy(1)-N(9)	145.6(3)	O(50)-Dy(4)-O(57)	145.06(19)

O(50)-Dy(1)-N(9)	126.1(2)	O(58)-Dy(4)-O(56)	70.9(2)
O(61)-Dy(1)-N(9)	77.1(3)	O(59)-Dy(4)-O(56)	143.21(19)
O(22)-Dy(1)-N(9)	62.3(2)	O(51)-Dy(4)-O(56)	77.0(2)
O(23)-Dy(2)-O(21)	113.6(3)	O(60)-Dy(4)-O(56)	132.2(2)
O(23)-Dy(2)-O(50)	88.9(3)	O(55)-Dy(4)-O(56)	61.3(2)
O(21)-Dy(2)-O(50)	156.1(2)	O(57)-Dy(4)-O(56)	76.80(19)
O(23)-Dy(2)-O(51)	157.4(2)	O(43)-Dy(5)-O(58)#2	136.1(2)
O(21)-Dy(2)-O(51)	87.3(2)	O(43)-Dy(5)-O(1)	87.5(2)
O(50)-Dy(2)-O(51)	71.9(2)	O(58)#2-Dy(5)-O(1)	122.3(2)
O(23)-Dy(2)-O(22)	74.5(2)	O(43)-Dy(5)-O(57)	108.1(2)
O(21)-Dy(2)-O(22)	126.1(2)	O(58)#2-Dy(5)-O(57)	72.22(19)
O(50)-Dy(2)-O(22)	65.9(2)	O(1)-Dy(5)-O(57)	138.3(2)
O(51)-Dy(2)-O(22)	86.6(2)	O(43)-Dy(5)-O(55)#2	74.8(2)
O(23)-Dy(2)-O(44)	125.3(2)	O(58)#2-Dy(5)-O(55)#2	73.70(19)
O(21)-Dy(2)-O(44)	75.2(2)	O(1)-Dy(5)-O(55)#2	90.5(2)
O(50)-Dy(2)-O(44)	85.3(2)	O(57)-Dy(5)-O(55)#2	130.54(19)
O(51)-Dy(2)-O(44)	66.3(2)	O(43)-Dy(5)-O(59)	149.4(2)
O(22)-Dy(2)-O(44)	145.80(19)	O(58)#2-Dy(5)-O(59)	74.4(2)
O(23)-Dy(2)-N(13)	74.5(3)	O(1)-Dy(5)-O(59)	69.7(2)
O(21)-Dy(2)-N(13)	69.1(3)	O(57)-Dy(5)-O(59)	79.3(2)
O(50)-Dy(2)-N(13)	127.8(2)	O(55)#2-Dy(5)-O(59)	123.6(2)
O(51)-Dy(2)-N(13)	107.6(2)	O(43)-Dy(5)-O(60)	94.2(2)
O(22)-Dy(2)-N(13)	62.1(2)	O(58)#2-Dy(5)-O(60)	123.86(18)
O(44)-Dy(2)-N(13)	144.2(3)	O(1)-Dy(5)-O(60)	71.7(2)
O(23)-Dy(2)-N(31)	67.7(3)	O(57)-Dy(5)-O(60)	68.81(18)
O(21)-Dy(2)-N(31)	76.5(3)	O(55)#2-Dy(5)-O(60)	159.68(19)
O(50)-Dy(2)-N(31)	106.8(3)	O(59)-Dy(5)-O(60)	60.1(2)
O(51)-Dy(2)-N(31)	128.5(2)	O(43)-Dy(5)-O(56)#2	68.6(2)
O(22)-Dy(2)-N(31)	141.7(3)	O(58)#2-Dy(5)-O(56)#2	69.5(2)
O(44)-Dy(2)-N(31)	62.3(2)	O(1)-Dy(5)-O(56)#2	145.4(2)
N(13)-Dy(2)-N(31)	111.3(3)	O(57)-Dy(5)-O(56)#2	74.87(19)
O(56)-Dy(3)-O(52)	146.7(3)	O(55)#2-Dy(5)-O(56)#2	60.1(2)
O(56)-Dy(3)-O(43)#1	70.5(2)	O(59)-Dy(5)-O(56)#2	140.45(19)
O(52)-Dy(3)-O(43)#1	136.2(2)	O(60)-Dy(5)-O(56)#2	132.2(2)
O(56)-Dy(3)-O(55)	62.0(2)	O(57)#2-Dy(6)-O(57)	117.44(8)
O(52)-Dy(3)-O(55)	134.7(2)	O(57)#2-Dy(6)-O(57)#1	117.43(8)

O(43)#1-Dy(3)-O(55)	73.6(2)	O(57)-Dy(6)-O(57)#1	117.43(8)
O(56)-Dy(3)-O(53)	110.9(2)	O(57)#2-Dy(6)-O(58)#2	76.2(2)
O(52)-Dy(3)-O(53)	71.7(3)	O(57)-Dy(6)-O(58)#2	73.91(19)
O(43)#1-Dy(3)-O(53)	71.6(2)	O(57)#1-Dy(6)-O(58)#2	147.2(2)
O(55)-Dy(3)-O(53)	144.6(2)	O(57)#2-Dy(6)-O(58)#1	73.91(19)
O(56)-Dy(3)-O(51)	76.97(19)	O(57)-Dy(6)-O(58)#1	147.2(2)
O(52)-Dy(3)-O(51)	80.6(2)	O(57)#1-Dy(6)-O(58)#1	76.2(2)
O(43)#1-Dy(3)-O(51)	143.1(2)	O(58)#2-Dy(6)-O(58)#1	80.0(2)
O(55)-Dy(3)-O(51)	76.2(2)	O(57)#2-Dy(6)-O(58)	147.2(2)
O(53)-Dy(3)-O(51)	138.4(2)	O(57)-Dy(6)-O(58)	76.2(2)
O(56)-Dy(3)-O(54)	73.7(3)	O(57)#1-Dy(6)-O(58)	73.91(19)
O(52)-Dy(3)-O(54)	76.8(3)	O(58)#2-Dy(6)-O(58)	80.0(2)
O(43)#1-Dy(3)-O(54)	111.1(3)	O(58)#1-Dy(6)-O(58)	80.0(2)
O(55)-Dy(3)-O(54)	131.1(2)	O(57)#2-Dy(6)-O(64)	80.69(15)
O(53)-Dy(3)-O(54)	69.3(3)	O(57)-Dy(6)-O(64)	80.69(15)
O(51)-Dy(3)-O(54)	74.6(3)	O(57)#1-Dy(6)-O(64)	80.69(15)
O(56)-Dy(3)-O(44)	121.5(2)	O(58)#2-Dy(6)-O(64)	132.09(15)
O(52)-Dy(3)-O(44)	68.1(2)	O(58)#1-Dy(6)-O(64)	132.09(15)
O(43)#1-Dy(3)-O(44)	119.7(2)	O(58)-Dy(6)-O(64)	132.08(15)

Symmetry transformations used to generate equivalent atoms: #1  $-y+1, x-y+1, z$ ; #2  $-x+y, -x+1, z$

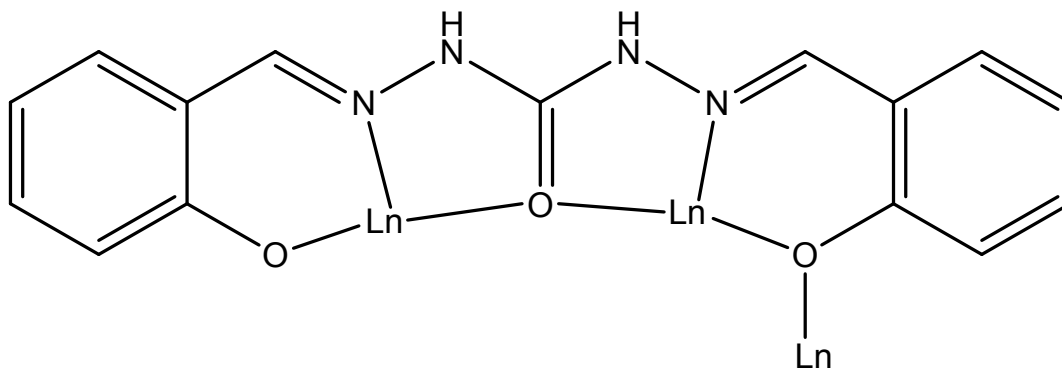


**Figure S1** Coordination mode of  $\text{bsc}^{2-}$  ligands in **1** and **2** ( $\text{Ln} = \text{Gd}^{\text{III}}$ , **1**;  $\text{Dy}^{\text{III}}$ , **2**).

**Table S6** SHAPE analysis for all nine-coordinate metals in **1** and **2**.

Geometry	CShM for Gd1	CShM for Gd3	CShM for Dy1	CShM for Dy3
EP-9	35.566	36.654	35.645	36.778
OPY-9	22.153	22.361	22.135	22.375
HBPY-9	18.266	18.185	18.093	18.260
JTC-9	15.036	16.313	15.199	16.510
JCCU-9	8.986	8.644	8.800	8.778
CCU-9	7.929	7.563	7.780	7.691
JCSAPR-9	1.398	1.316	1.326	1.296
<b>CSAPR-9</b>	<b>0.626</b>	<b>0.523</b>	<b>0.591</b>	<b>0.487</b>
JTCTPR-9	2.544	3.314	2.662	3.166
TCTPR-9	1.409	1.479	1.519	1.382
JTDIC-9	12.512	12.860	12.462	12.991
HH-9	11.553	12.144	11.813	12.164
MFF-9	1.171	1.094	1.203	1.097

SHAPE code: EP-9, enneagon; OPY-9, octagonal pyramid; HBPY-9, heptagonal bipyramid; JTC-9, Johnson triangular cupola J3; JCCU-9, capped cube J8; CCU-9, spherical-relaxed capped cube; JCSAPR-9, capped square antiprism J10; CSAPR-9, spherical capped square antiprism; JTCTPR-9, tricapped trigonal prism J51; TCTPR-9, spherical tricapped trigonal prism; JTDIC-9, tridiminished icosahedron J63; HH-9, hula-hoop; MFF-9, muffin.

**Table S7** SHAPE analysis for all eight-coordinate metals in **1** and **2**.

Geometry	CShM for Gd2	CShM for Gd4	CShM for Gd6	CShM for Dy2	CShM for Dy4	CShM for Dy5
OP-8	30.867	24.269	23.625	30.679	23.741	24.469
HPY-8	22.894	21.842	23.678	22.786	23.811	21.920
HBPY-8	12.841	16.304	14.613	13.005	14.574	16.139
CU-8	9.741	11.688	9.332	9.813	9.160	11.455
<b>SAPR-8</b>	5.242	<b>1.786</b>	<b>1.167</b>	5.094	<b>1.163</b>	<b>1.715</b>
<b>TDD-8</b>	<b>3.826</b>	2.995	2.211	<b>3.700</b>	2.147	2.872
JGBF-8	11.605	15.478	14.466	11.792	14.549	15.357
JETBPY-8	19.933	23.616	24.879	20.020	24.976	23.915
JBTPR-8	5.015	2.673	2.778	4.918	2.805	2.577
BTPR-8	4.349	2.140	2.046	4.258	2.098	2.075
JSD-8	6.560	5.073	4.898	6.551	4.848	5.011
TT-8	9.815	12.486	10.110	9.887	9.952	12.261
ETBPY-8	14.777	20.308	21.531	14.898	21.640	20.630

SHAPE codes: OP-8, octagon; HPY-8, heptagonal pyramid; HBPY-8, hexagonal bipyramid; CU-8, cube; SAPR-8, square antiprism; TDD-8, triangular dodecahedron; JGBF-8, Johnson gyrobifastigium J26; JETBPY-8, Johnson elongated triangular bipyramid J14; JBTPR-8, biaugmented trigonal prism J50; BTPR-8, biaugmented trigonal prism; JSD-8, snub diphenoid J84; TT-8, triakis tetrahedron; ETBPY-8, elongated trigonal bipyramid.

**Table S8** SHAPE analysis for all seven-coordinate metals in **1** and **2**.

Geometry	CShM for Gd5	CShM for Dy6
HP-7	37.352	37.281
HPY-7	18.450	18.561
PBPY-7	8.953	8.923
<b>COC-7</b>	<b>0.160</b>	<b>0.146</b>
CTPR-7	2.216	2.192
JPBPY-7	12.349	12.297
JETPY-7	19.857	19.779

SHAPE Codes: HP-7, heptagon; HPY-7, hexagonal pyramid; PBPY-7, pentagonal bipyramid; COC-7, capped octahedron; CTPR-7, capped trigonal prism; JPBPY-7, Johnson pentagonal bipyramid J13; JETPY-7, Johnson elongated triangular pyramid J7.

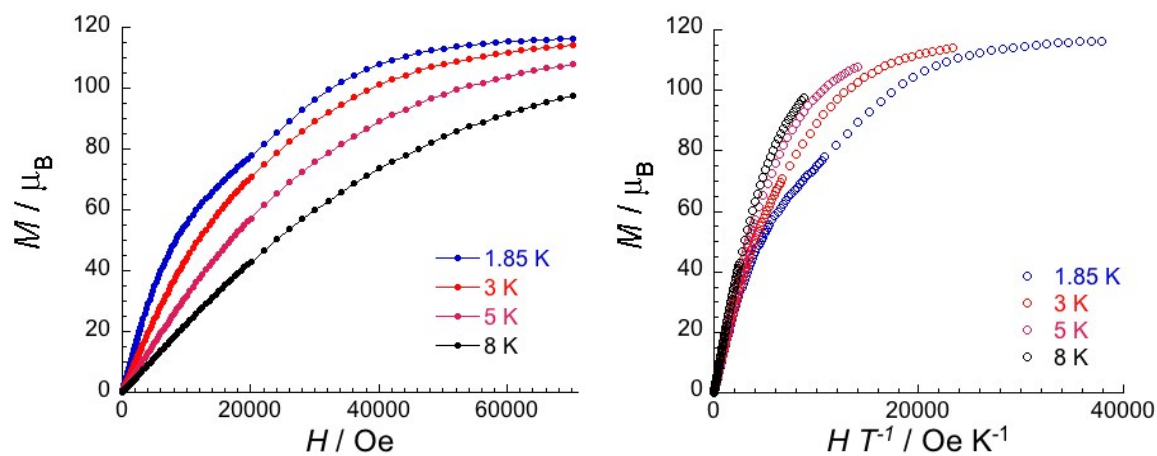


**Figure S2** Field dependence of the magnetization as  $M$  vs  $H$  (left) and  $M$  vs  $H/T$  (right) plots for **1** between 1.8 and 8 K with sweep-rates of 100 – 600 Oe/min. The solid lines are guides for the eyes.

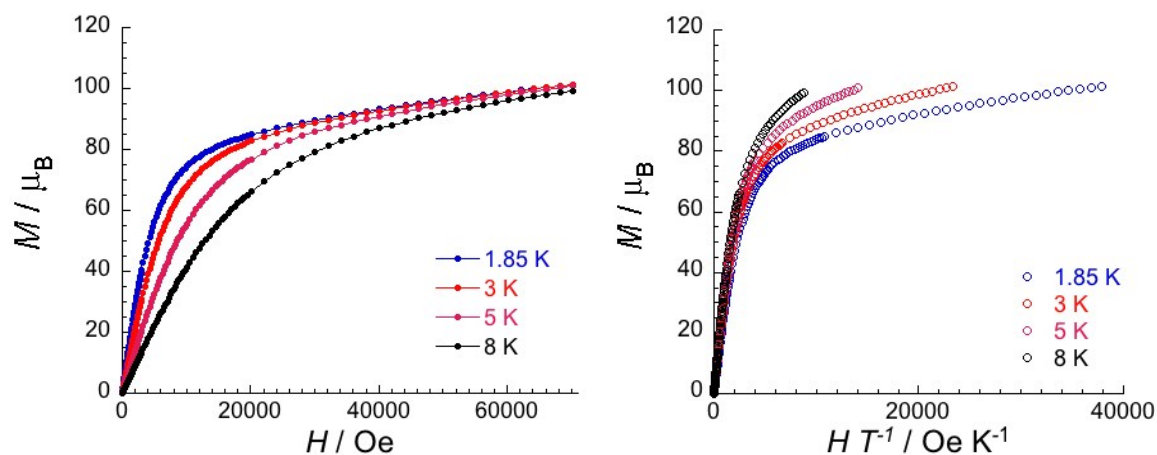


**Figure S3** Field dependence of the magnetization as  $M$  vs  $H$  (left) and  $M$  vs  $H/T$  (right) plots for **2** between 1.8 and 8 K with sweep-rates of 100 – 600 Oe/min. The solid lines are guides for the eyes.

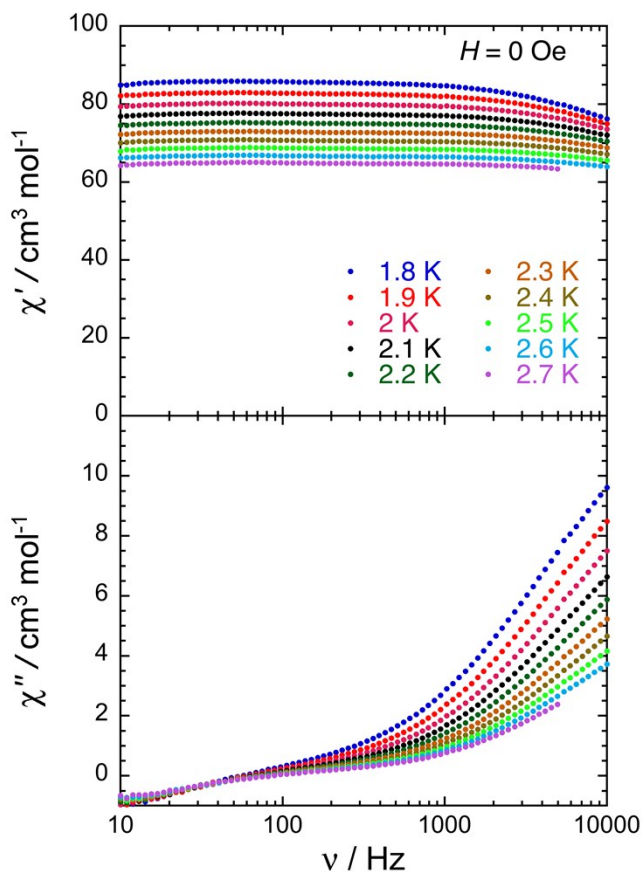


**Figure S4** Frequency dependence of the real ( $\chi'$ , top) and imaginary ( $\chi''$ , bottom) components of the ac susceptibility in zero-dc field at different temperatures between 1.8 and 2.7 K for a polycrystalline sample of **2**.

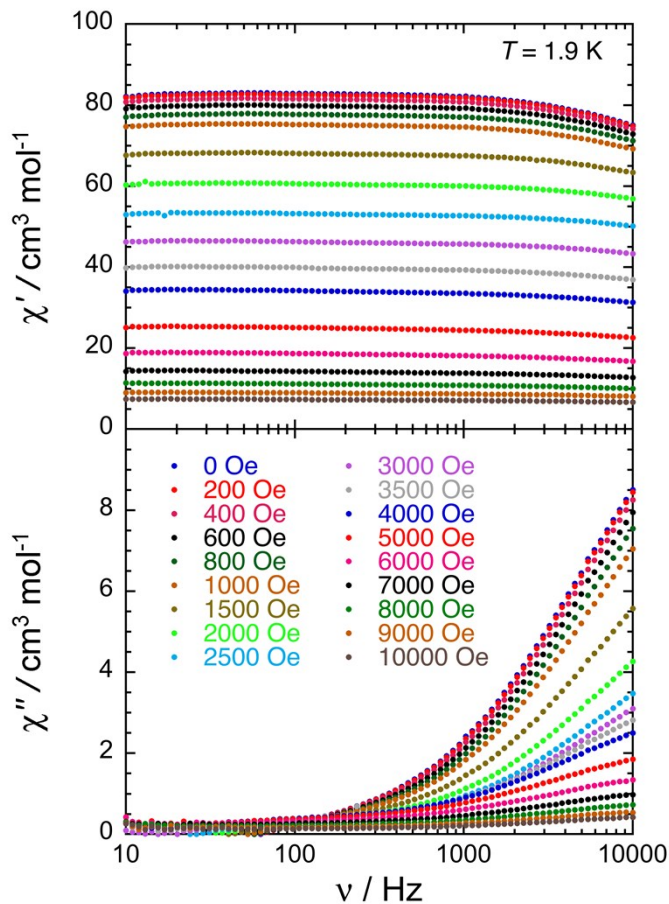


**Figure S5** Frequency dependence of the real ( $\chi'$ , top) and imaginary ( $\chi''$ , bottom) components of the ac susceptibility at 1.9 K at different dc fields between 0 and 1 T for a polycrystalline sample of **2**.

## References

1. D. Maity, A. K. Manna, D. Karthigeyan, T. K. Kundu, S. K. Pati and T. Govindaraju, *Chem. Eur. J.*, 2011, **17**, 11152.
2. Bruker, APEX2, 2012, Bruker AXS Inc., Madison, Wisconsin, USA.
3. Bruker, SADABS, 2003, Bruker AXS Inc., Madison Wisconsin, USA.
4. G. M. Sheldrick, *Acta Cryst.* 2015, **C71**, 3.
5. G. M. Sheldrick, *Acta Crystallogr. A*, 2008, **64**, 112.
6. A. L. Spek, *Acta Crystallogr. C*, 2015, **71**, 9.